



Since January 2020 Elsevier has created a COVID-19 resource centre with free information in English and Mandarin on the novel coronavirus COVID-19. The COVID-19 resource centre is hosted on Elsevier Connect, the company's public news and information website.

Elsevier hereby grants permission to make all its COVID-19-related research that is available on the COVID-19 resource centre - including this research content - immediately available in PubMed Central and other publicly funded repositories, such as the WHO COVID database with rights for unrestricted research re-use and analyses in any form or by any means with acknowledgement of the original source. These permissions are granted for free by Elsevier for as long as the COVID-19 resource centre remains active.



# Lopinavir-menthol co-crystals for enhanced dissolution rate and intestinal absorption

Noha D. Fayed<sup>\*</sup>, Mona F. Arafa, Ebtesam A. Essa, Gamal M. El Maghraby

Department of Pharmaceutical Technology, Faculty of Pharmacy, University of Tanta, Tanta, Egypt

## ARTICLE INFO

### Keywords:

Lopinavir  
Menthol  
Co-crystal  
Dissolution rate  
Intestinal permeability  
In situ

## ABSTRACT

Lopinavir is an antiretroviral, antiparasitic agent and recently utilized in treatment of COVID-19. Unfortunately, lopinavir exhibited poor oral bioavailability due to poor dissolution, extensive pre-systemic metabolism, and significant P-glycoprotein intestinal efflux. Accordingly, the aim was to enhance dissolution rate and intestinal absorption of lopinavir. This employed co-processing with menthol which is believed to modify crystalline structures and inhibit intestinal efflux. Lopinavir was mixed with menthol at different molar ratios before ethanol assisted kneading. Formulations were evaluated using FTIR spectroscopy, differential scanning calorimetry (DSC), X-ray powder diffraction (XRD) and dissolution studies. Optimum ratio was utilized to assess lopinavir intestinal permeability. This employed in situ rabbit intestinal perfusion technique. FTIR, DSC and XRD indicated formation of lopinavir-menthol co-crystals at optimum molar ratio of 1:2. Additional menthol underwent phase separation due to possible self-association. Co-crystallization significantly enhanced lopinavir dissolution rate compared with pure drug to increase the dissolution efficiency from 24.96% in case of unprocessed lopinavir to 91.43% in optimum formulation. Lopinavir showed incomplete absorption from duodenum and jejunum-ileum segments with lower absorptive clearance from jejunum-ileum reflecting P-gp efflux. Co-perfusion with menthol increased lopinavir intestinal permeability. The study introduced menthol as co-crystal co-former for enhanced dissolution and augmented intestinal absorption of lopinavir.

## 1. Introduction

Lopinavir is a protease inhibitor that has been widely used for many years as therapy for human immunodeficiency virus (HIV) infection in both adults and children. As antiretroviral therapy, lopinavir effectively inhibits viral replication and offers a higher quality of life for the patients [1–4]. Lopinavir is also used as a prophylactic treatment for pregnant HIV-mothers to protect their neonates [5,6]. Lopinavir has been shown to be safe for HIV-infected children with severe acute malnutrition [7]. Lopinavir exhibited an inhibition of growth of some fungal cells and has potential effect as a therapy for fungal infections [8, 9]. In addition, lopinavir has been investigated as a treatment plan for some parasitic infections [10,11]. Recently, lopinavir has been evaluated alone or in combination with ritonavir in the treatment of COVID patients, but limited success has been shown [12–15].

Lopinavir experiences extensive gastrointestinal (GI) and liver metabolism by the enzyme cytochrome P450 3A4 and is significantly affected by P-glycoprotein efflux. This in addition to its poor aqueous

solubility and slow dissolution (BCS class II) resulted in poor oral bioavailability of lopinavir [16–19]. Accordingly, lopinavir doesn't reach the therapeutic concentration in the blood stream. Fixed dose combinations of lopinavir and ritonavir are now commercially available to solve this bioavailability hassle. Ritonavir is an analogue to lopinavir that is also a protease inhibitor and when co-administered, enhances the absorption of lopinavir from the intestinal lumen to the systemic circulation by acting as a CYP3A4 and P-gp inhibitor, thereby boosting the oral bioavailability of lopinavir. However, the in-vivo action of ritonavir has been reported to be negligible, since lopinavir is ten times more potent than ritonavir which indicates that the lopinavir-ritonavir mixture in-vivo action is mainly contributed to lopinavir [20]. Moreover, the oral solution of lopinavir-ritonavir combination have a very bitter taste and contains high amount of alcohol that causes some GI side effects [2,4,21,22]. Therefore, it is certain that there is a need for a formulation that doesn't include ritonavir to improve the oral bioavailability of lopinavir.

Various pharmaceutical strategies have been employed to promote

<sup>\*</sup> Corresponding author.

E-mail addresses: [noha.fayed@pharm.tanta.edu.eg](mailto:noha.fayed@pharm.tanta.edu.eg) (N.D. Fayed), [mona.arafa@pharm.tanta.edu.eg](mailto:mona.arafa@pharm.tanta.edu.eg) (M.F. Arafa), [ebtesam.eisa@pharm.tanta.edu.eg](mailto:ebtesam.eisa@pharm.tanta.edu.eg) (E.A. Essa), [gamal.elmaghraby@pharm.tanta.edu.eg](mailto:gamal.elmaghraby@pharm.tanta.edu.eg) (G.M. El Maghraby).

<https://doi.org/10.1016/j.jddst.2022.103587>

Received 6 April 2022; Received in revised form 27 June 2022; Accepted 8 July 2022

Available online 11 July 2022

1773-2247/© 2022 Elsevier B.V. All rights reserved.

lopinavir as a single therapy for HIV, increase its solubility, dissolution, and hence enhance its oral bioavailability without the need for ritonavir. These included amorphous solid dispersion [12,23]. In addition, freeze-dried formulations reported higher lopinavir oral bioavailability [2,24]. Amino acid prodrugs of lopinavir were also investigated for their potential to evade P-glycoprotein efflux pump and the extensive first pass effects [18].

Crystalline structure modification has been shown to enhance the dissolution rate of drugs. The crystalline structure modification involved amorphization, co-crystallization or formulation of eutectic mixture [25–28]. Co-crystals and eutectics are considered as non-covalent derivatives and can be developed by co-processing drugs with benign co-formers. A eutectic mixture develops if the cohesive forces dominate and results in formation of new crystalline species with reduced melting point. This is expected to weaken the crystalline structure resulting in enhanced dissolution rate. It is also believed that reduction of melting point can augment lipid solubility. Furthermore, the eutectic mixture has many advantages since its preparation is fairly inexpensive, and the formed compound is crystalline offering better stability compared to amorphous compounds [27,29–32].

Co-crystallization result when the adhesive forces between the drug and co-former dominate [33–35]. The mechanochemical approach is the most commonly employed strategy for formation of co-crystals. The task is to develop supramolecular mixing of solids using either neat grinding or liquid assisted grinding [36]. Co-crystallization was successfully adopted to enhance the dissolution rate of a variety of poorly soluble drugs [25,26]. The benefit will be augmented if the selected excipient was able to enhance the biopharmaceutical properties of drugs.

Menthol is believed to enhance the membrane permeability of drugs probably by fluidization of membrane lipids in addition to potential inhibition of P-glycoprotein efflux transporters [19,37–41]. Menthol was shown to develop eutectic mixture or co-crystals [42,43].

Accordingly, the objective of this study was to investigate the effect of co-processing of lopinavir with menthol on the crystalline structure, dissolution rate and intestinal permeability of lopinavir.

## 2. Materials and methods

### 2.1. Materials

Lopinavir was purchased from Haihang Industry Co., Ltd, China. Pharmaceutical grade potassium dihydrogen phosphate, potassium hydroxide, ortho-phosphoric acid, potassium chloride, disodium hydrogen phosphate, sodium chloride and tween 80 were procured from El Nasr Pharmaceuticals Chemicals Co., Cairo, Egypt. Acetonitrile (HPLC grade) was obtained from Fisher Scientific UK, Loughborough, Leicis, United Kingdom. L-menthol was obtained from Bhagat Aromatics Ltd, India. PEG 200 was purchased from Sigma Aldrich, Steinheim, Germany. Avicel (PH 102) and aerosil 200 were kindly donated by Sigma Pharmaceutical Co., Quesna, Egypt.

### 2.2. Preparation of co-crystals

Mixtures of lopinavir and menthol at molar ratios of 1:1, 1:1.5, 1:2, and 1:3 were fabricated. The actual composition of the prepared

**Table 1**  
The composition of the tested formulations.

Formulation	Lopinavir (mg)	Menthol (mg)	Avicel (mg)	Aerosil (mg)
<b>Lop: Menth 1:1</b>	628.8	156.3	1257.6	139.7
<b>Lop: Menth 1:1.5</b>	628.8	234.4	1257.6	139.7
<b>Lop: Menth 1:2</b>	628.8	312.67	1257.6	139.7
<b>Lop: Menth 1:3</b>	628.8	468.9	1257.6	139.7

formulations is presented in Table 1 as weight ratios. For dissolution studies, the formulations included avicel and aerosil which were added to prevent formation of sticky aggregates. The mixtures were prepared using ethanol assisted kneading technique [44]. Briefly, lopinavir and menthol were mixed in a mortar and ethanol was added dropwise with continuous grinding to form a smooth paste. The paste was subjected to continuous grinding until evaporation of ethanol. The process of paste formation was repeated and avicel/aerosil mixture was added gradually with mixing. Mixing process continued until evaporation of the organic solvent and development of flowable powder. The developed system was left at ambient conditions (25 °C) for an overnight.

### 2.3. Determination of drug content

Known weight of the tested formulation equivalent to 50 mg of lopinavir was dissolved in ethanol and suitably diluted with dissolution medium before drug quantification using HPLC method. These procedures were repeated in triplicates. The following equation was utilized for calculating the drug content in each formulation:

$$\text{Drug content (\%)} = (\text{Recovered amount} / \text{Theoretical amount}) \times 100 \quad 100$$

### 2.4. High pressure liquid chromatography

High pressure liquid chromatographic method was employed for quantification of lopinavir. The utilized chromatographic system (1260 infinity, DE, Germany) was a product of Agilent technologies. This system was supported with variable wavelength UV detector (VWD 1260) which was adjusted at wavelength of 210 nm for quantitative measurement of lopinavir concentration in the tested samples. The sampling system (TCC 1260) was automatic and fully computerized system. A reversed phase column (Intersil® C18 column, 150 mm × 4.6 mm (i.d.) with an average particle size of 5 µm produced by GL Sciences Inc., Tokyo, Japan) was used as the stationary phase. Samples containing lopinavir (30 µl) were injected into the system during the isocratic flow of the mobile phase which comprised 0.02 Molar potassium dihydrogen phosphate buffer adjusted to pH 6.8 and acetonitrile at a ratio of 25:75. The software (Agilent OpenLAB ChemStation) was employed in data analysis.

### 2.5. Fourier's transform infrared spectroscopy (FTIR)

The FTIR spectral patterns of pure unprocessed lopinavir, menthol and the tested formulations were examined using the spectrophotometer (Bruker Tensor 27, Germany) which was equipped with DLATGS detector (Ettlingen, Germany). This was done to assess any changes in the spectral pattern of the main functional groups after processing that can indicate possible interaction and formation of new species. The tested sample was mixed with spectroscopic grade potassium bromide and was compressed using hydraulic press into solid disks. Sample scan was performed in the range of 4000 to 400 cm<sup>-1</sup>. Opus IR (FTIR spectroscopy) software was adopted for data curation.

### 2.6. Differential scanning calorimetry (DSC)

The thermal behavior of lopinavir and menthol both as pure entities and co-processed form were investigated using the differential scanning calorimeter (Discovery DSC 25-TA instrument, Newcastle, DE, USA). Known weight of the tested sample was packed in an aluminum pan, which was occluded with its lid, and was finally crimped. The crimped pan was placed in the sample holder and an empty one was employed as reference. The thermogram was recorded by heating the sample at a rate of 10 °C/min starting from 20 to 400 °C. This process was operated under continuous and constant flow of nitrogen gas (50 ml/min). The

recorded data were curated using TRIOS software. The thermal parameters including transition midpoint (T<sub>m</sub>) and enthalpy were assessed for each transition peak.

## 2.7. X-ray powder diffraction (XRPD)

The X-ray diffraction pattern and crystallinity of lopinavir, menthol and the fabricated mixtures were evaluated using PAN analytical X-Ray diffractometer (model X'Pert PRO, Philips, Amsterdam, Netherlands). This X-Ray diffractometer is supported with secondary monochromator, Cu-K $\alpha$  radiation ( $\lambda = 1.542 \text{ \AA}$ ). The monochromator was operated at current of 35 mA and 45 KV. The equipment was supplied with X'Celerator detector that enables data collection. Sample scan was performed with continuous scan mode at ambient temperature using 2 theta scan axis. The scanning was recorded in the range of 3–60°, operating the system at scanning step size of 0.03°.

## 2.8. Dissolution studies

In order to assess the impact of lopinavir wet co-processing with menthol on its dissolution rate, the dissolution studies were performed. The study employed USP 2 dissolution apparatus (paddle type) which is a product of Copley Scientific Dis 6000, Nottingham, UK. The test was performed in 900 ml dissolution medium comprising 1% w/v Tween 80 solution in 0.01 M phosphate buffer (pH 6.8). The temperature of the dissolution medium was adjusted at  $37 \pm 0.5 \text{ }^\circ\text{C}$  to mimic the in vivo condition. The tested sample (400 mg of lopinavir or its equivalent) was added to the dissolution vessel and the paddle of the apparatus was rotated at speed of 50 rpm. At fixed time intervals (5, 10, 15, 30, 45, and 60 min), samples (5 ml) were withdrawn, and were immediately filtered by 0.45  $\mu\text{m}$  Millipore filter. After sample withdrawal, equivalent volume of the fresh dissolution media was added to keep on the constant volume for maintaining sink conditions. The developed high pressure liquid chromatographic method was employed to determine lopinavir concentration in the dissolution samples. Dissolution study for each formulation was conducted in triplicates. After measuring lopinavir concentration in the dissolution samples, the cumulative amounts of lopinavir dissolved were computed as percentage of the load and plotted against the time to generate dissolution profiles. Utilizing the generated profiles, the amount of drug dissolved within the first 5 min (%Q5) and the dissolution efficiency (% DE) were calculated. The nonlinear trapezoidal rule was employed in the estimation of the dissolution efficiency [45]. These parameters were used to compare between different formulations. Further comparison between the overall dissolution profiles was achieved using the similarity factor test [46].

## 2.9. In-situ perfusion model

### 2.9.1. In-situ intestinal perfusion studies

The well established in-situ rabbit intestinal perfusion was adopted to assess the intestinal permeability of lopinavir. Firstly, perfusion solution of lopinavir containing 30  $\mu\text{g/ml}$  was prepared in phosphate buffered saline (containing 10% v/v polyethylene glycol 200). This was prepared both in absence and presence of menthol which was included at 1:2 molar ratio of lopinavir to menthol. These solutions were used to investigate the effect of menthol on intestinal absorption of lopinavir. The tested solutions were freshly prepared just before the experiment. The perfusion solution containing lopinavir and menthol was prepared at the optimum molar ratio of co-crystallization which produced the best dissolution pattern. This composition is expected to mimic the composition of drug solution after dissolution in presence of menthol.

### 2.9.2. Segment preparation

Segment preparation is well documented in literature [47–49]. Briefly, anesthesia was achieved by IM administration of chlorpromazine HCl (2 mg/kg) as to provide muscle relaxation before

injection of ketamine HCl in 2 doses of 45 mg/kg given at 15 min interval and another dose of 25 mg/kg may be required.

The anesthetized rabbit was fixed in supine position on thermostated matrix before shaving the abdominal hair and making a midline incision (6–8 cm length). The required intestinal segment was uncovered. The desired length of tested intestinal segment was measured and tied from both sides with surgical threads then they were cannulated. This length used depended on the segment; 15 cm for duodenum, and 30 cm for jejunum-ileum. Normal saline maintained at 37  $^\circ\text{C}$  was utilized to clean the desired segment.

### 2.9.3. Experimental design

The study protocol was approved by the Faculty of Pharmacy, Tanta University Ethical Committee (Approval number, 1822017). The study employed 6 male albino rabbits weighing  $2 \pm 0.11 \text{ kg}$ . Rabbits were divided into 2 groups. The first group comprised 3 rabbits which were utilized to investigate the duodenal and jejunum-ileal absorption of lopinavir in absence of menthol. The second group of animals (3 rabbits) was employed to assess the effect of menthol on the intestinal membrane transport parameters of lopinavir.

### 2.9.4. In-situ intestinal perfusion

The tested lopinavir solutions prepared in phosphate buffered saline were pumped at a rate of 0.27 ml/min using constant rate perfusion pump (Harvard Apparatus-22, Millis, MA, USA). The samples eluted from the investigated segment were gathered every 10 min for 2 h in stoppered tubes with a known weight. After that, the tubes were weighed again to determine the effluent weight, which is the difference in tube weight before and after sample collection.

### 2.9.5. Sample analysis

For quantification of the lopinavir concentration in perfusate samples using the developed HPLC assay method, the samples were treated as follow. First, the samples were centrifuged then 1 ml of the supernatant was diluted 1 in 4 with phosphate buffered saline free from PEG 200 before injection into the HPLC for drug assay.

### 2.9.6. Data analysis

**2.9.6.1. Absorptive clearance.** The amount of lopinavir in each sample ( $C_{\text{out}}$ ) was calculated by correcting the recovered concentration to the net water flux. The ratio between  $C_{\text{out}}$  and the amount of lopinavir perfused ( $C_{\text{in}}$ ) produces the fraction of lopinavir remaining after perfusion. The fraction remaining at steady state  $\{(C_{\text{out}}/C_{\text{in}})_{\text{ss}}\}$  was taken from the average of the fractions remaining in samples collected during the second hour of perfusion. This was used to calculate the absorptive clearance (PeA) which was expressed as ml/minute using equation (1), in which A is the effective surface area ( $\text{cm}^2$ ), Pe is apparent permeability coefficient ( $\text{cm/min}$ ), and Q is the average flow rate of the perfusate through the target segment ( $\text{ml/min}$ ).

$$\text{PeA} = -Q * \ln \{C_{\text{(out)}}/C_{\text{(in)}}\}_{\text{ss}} \quad (1)$$

The fraction of the drug absorbed at steady state ( $F_a$ ) was calculated using equation (2).

$$F_a = 1 - \{C_{\text{(out)}}/C_{\text{(in)}}\}_{\text{ss}} = 1 - \exp^{-(\text{PeA}/Q)} \quad (2)$$

The length of the intestine remaining after complete drug absorption is described as the anatomical reserve length (ARL) and was computed using equation (3) in which  $L^*$  is the physiological length of the selected intestinal segment in centimeters and  $l^*$  (cm) is the length needed for complete absorption of drug.

$$\text{ARL} = (L^*) - (l^*) \quad (3)$$

Basically, lopinavir cannot disappear completely from the intestinal lumen particularly in a logarithmic situation. Thus, a 5% fraction was

suggested to stay with 95% absorption being considered as an approximation of complete absorption. The length needed for 95% absorption (L95%) was thus computed using equation (4).

$$0.05 = \exp^{-((PeA \cdot l^*)/Q)} \quad (4)$$

Where PeA is absorptive clearance normalized to length and  $l^*$  is L95% for the given drug.

**2.9.6.2. Effect of water flux on intestinal absorption.** Lopinavir absorption was assessed as a function of water flux by plotting the absorptive clearance as a function of net water flux  $J_w$  (ml/min) which was computed from the difference between the volume of the perfusate pumped during a given time period ( $Q_{in}$ ) and the volume of perfusate recovered from the segment during this time ( $Q_{out}$ ). This is simplified by equation (5).

$$J_w = Q_{in} - Q_{out} \quad (5)$$

The rate of drug absorption ( $J_s$ ) in  $\mu\text{g}/\text{min}$  results from diffusive and convective processes. The net amount of drug absorbed per unit time can be deduced from equation (6).

$$J_s = K_s (C - C_p) + \emptyset_s J_w C \quad (6)$$

Where the diffusive process is described by  $[K_s (C - C_p)]$  in which  $K_s$  is the diffusive permeability coefficient of the drug. The concentration of the drug in the intestinal lumen is expressed as  $C$  with that in the plasma being defined as  $C_p$  and the convective process is represented by  $[\emptyset_s J_w C]$  in which  $\emptyset_s$  is the sieving coefficient of drug. Equation (6) can be approximated to equation (7) at steady state, taking into consideration the existence of sink conditions in blood.

$$J_{ss} = DAKp / \Delta x (C_{ss}) + \emptyset_s J_w (C_{ss}) \quad (7)$$

"Where  $J_{ss}$  is the steady state solute flux ( $\mu\text{g}/\text{min}$ ),  $D$  is the diffusion coefficient of the drug,  $A$  is the effective surface area of drug absorption  $K_p$  is the (octanol/water) partition coefficient of the compound.  $\Delta x$  is the path length.  $C_{ss}$  is the length averaged steady state concentration of the solute in the lumen ( $\mu\text{g}/\text{ml}$ ). Rearrangement of equation (7) gives":

$$J_{ss}/C_{ss} = DAKp / \Delta x + \emptyset_s J_w \quad (8)$$

The term  $J_{ss}/C_{ss}$  is the overall absorptive clearance (ml/min) and can be practically calculated as permeability surface area product, PeA. When PeA is dependent on the water flux, the absorption mechanisms include a paracellular component. On the other hand, if the permeability coefficient term ( $DAKp/\Delta x$ ) is different from zero, this reflects a role for transcellular absorption.

## 2.10. Statistical analysis

In vitro and in-situ data were subjected for statistical analysis to assess the significance of the effect of co-processing of lopinavir with menthol on the dissolution rate and intestinal permeability of lopinavir. This was achieved using the Kruskal Wallis test followed by Tukey's multiple comparisons as post hoc analysis employing IBM SPSS 16 software.

Dissolution profiles were also compared using similarity factor test which computes the F2 value that must be less than 50% for the dissolution profiles to differ significantly [27].

## 3. Results and discussion

### 3.1. Characterization of the prepared formulations

#### 3.1.1. Drug content

The lopinavir drug content values were determined to be  $104.7\% \pm 1.3$ ,  $105.6\% \pm 1.2$ ,  $103.3\% \pm 1.3$  and  $115.4\% \pm 3.2$  respectively for

formulations containing lopinavir with menthol at molar ratios of 1:1, 1:1.5, 1:2, and 1:3. The closeness of the calculated drug content values to 100% in addition to the small SD reflects the homogeneity of the prepared mixtures.

#### 3.1.2. FTIR spectroscopy

Spectral pattern for pure lopinavir was recorded to assess possible interaction after co-processing with menthol at different molar ratios. The FTIR spectrum of lopinavir showed the main characteristic peaks that correspond to its different functional groups (Fig. 1). The peak recorded at  $3402 \text{ cm}^{-1}$  and  $3300 \text{ cm}^{-1}$  can be assigned to both OH and N-H stretching vibration. The sharpness of the absorption band of the OH group reflects its freedom. The C-H aromatic and aliphatic were noted as a band starts from  $2864$  to  $3066 \text{ cm}^{-1}$ . The C=O of the primary and secondary amides were recorded as strong peaks at  $1604$  and  $1514 \text{ cm}^{-1}$  respectively. The stretching peak of C-N was evident at  $1448 \text{ cm}^{-1}$  and C-O stretching vibrations (asymmetric and symmetric) were recorded as multiple peaks at  $1240$ ,  $1197$ ,  $1093$  and  $1050 \text{ cm}^{-1}$ . Similar FTIR spectrum for lopinavir was reported by various investigators [20, 50].

The FTIR spectrum of menthol showed the characteristic phenolic O-H stretching vibration as a broad peak at  $3416 \text{ cm}^{-1}$ . The stretching vibration for the aromatic and the aliphatic C-H were observed in the range of  $2870$ – $2957 \text{ cm}^{-1}$ . The isopropyl group stretching vibration was noted at  $1380 \text{ cm}^{-1}$  (Fig. 1). All these characteristic peaks were recorded previously for pure menthol [51–53].

The FTIR spectrum of the prepared formulations showed a summation of the main peaks that were recorded for lopinavir and menthol except for the absorption band of the NH group which showed broadening and shifting to lower wave number (Fig. 1). This suggests possible hydrogen bonding. This effect might imply possible transformation in the crystalline structure which is to be verified by other instrumental techniques in the proceeding sections.

#### 3.1.3. Differential scanning calorimetry (DSC)

The changes in the thermal behavior of lopinavir after wet grinding with menthol at different molar ratios were monitored using DSC. The recorded thermal patterns are shown in Fig. 2. These thermographs were employed to calculate the thermodynamic parameters which are presented Table 2.

For pure unprocessed lopinavir, the recorded thermogram showed broad asymmetric endothermic peak with apex being towards the higher temperature. This endotherm has an onset of  $104 \text{ }^\circ\text{C}$  and end-set of  $126.8 \text{ }^\circ\text{C}$  with the apex being recorded at  $121 \text{ }^\circ\text{C}$ . This endotherm can be attributed to melting of lopinavir. Another broad exothermic peak was shown at  $T_m$  of  $340.1 \text{ }^\circ\text{C}$  which can be attributed to lopinavir decomposition events (Fig. 2). Similar thermal behavior was reported previously for lopinavir [20,54,55].

The thermogram of menthol showed two successive endothermic peaks. The first of which was shown at  $T_m$  value of  $49 \text{ }^\circ\text{C}$  (onset at  $44.2 \text{ }^\circ\text{C}$  and end-set at  $56.6 \text{ }^\circ\text{C}$ ). This peak was accredited to menthol melting. The second endotherm was detected at  $172.8 \text{ }^\circ\text{C}$  and was credited to complete thermal decomposition of menthol. The same thermal behavior of menthol was stated in literature [37,51–56].

Wet co-grinding of lopinavir with menthol resulted in significant modulation in the recorded thermal pattern regardless the molar ratio used. The thermograms showed sharp symmetric endothermic peak at  $119.8 \text{ }^\circ\text{C}$ . This sharp endotherm was recorded in all tested molar ratios of lopinavir to menthol but with different enthalpy. The enthalpy of the recorded endotherm increases with increasing menthol concentration in the system up to 1:2 M ratio (lopinavir to menthol). This modulation was accompanied by complete disappearance of melting transition endotherm of menthol. Further increase in menthol reduced the enthalpy of this endotherm and was associated with the appearance of an endothermic peak at  $40 \text{ }^\circ\text{C}$  which can be attributed to excess menthol which underwent phase separation in formulation containing lopinavir with

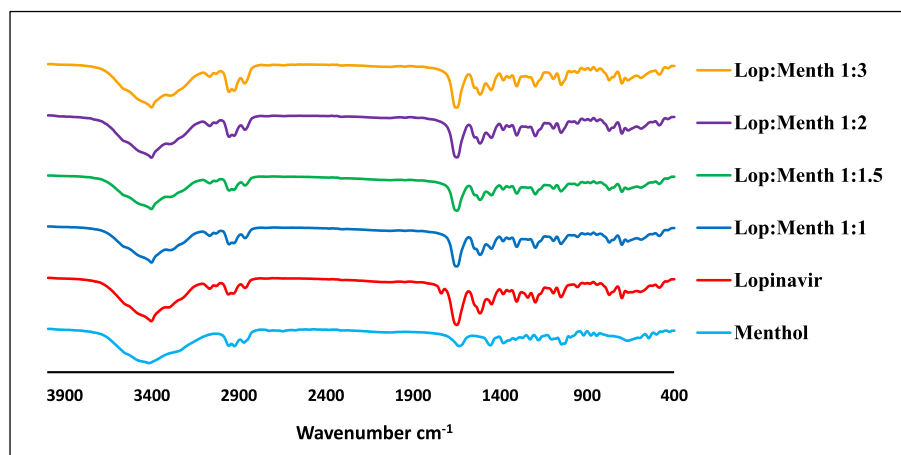


Fig. 1. FTIR spectra of menthol, pure lopinavir, and formulations containing lopinavir and menthol at molar ratios of 1:1,1:1.5, 1:2, and 1:3.

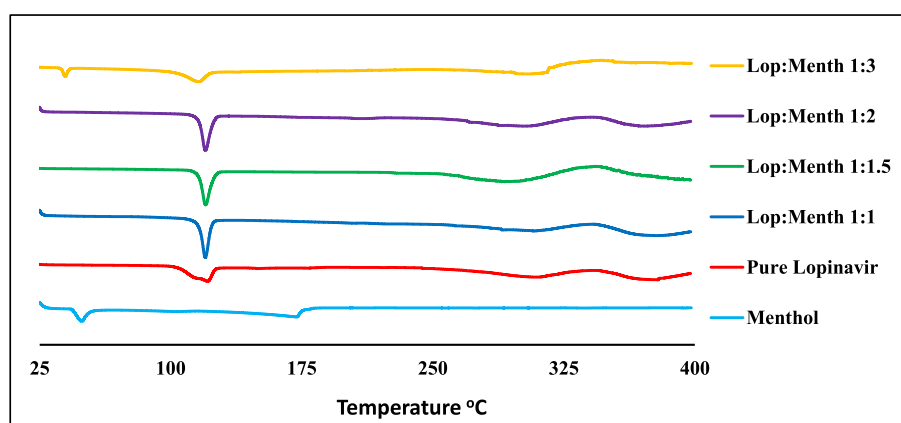


Fig. 2. Representative DSC thermograms of menthol, pure lopinavir, and formulations containing lopinavir and menthol at molar ratios of 1:1,1:1.5, 1:2, and 1:3.

Table 2

The thermodynamic parameters calculated from thermal analysis of lopinavir before and after co-processing with menthol.

Formulation	Onset (°C)	End-set (°C)	T <sub>m</sub> (°C)	Enthalpy ΔH (J/g)
Pure Lopinavir	104	126.8	121	38.6
Pure Menthol	44.2	56.6	49	15.36
Lop: Menth 1:1	122	181.5	172.8	30.86
Lop: Menth 1:1.5	110.8	126.8	119.8	45.84
Lop: Menth 1:2	112.3	126.8	119.9	55.16
Lop: Menth 1:3	112	128.6	119.8	59
Lop: Menth 1:3	111.54	128	119.7	33.9

menthol at molar ratio of 1:3. The T<sub>m</sub> of the decomposition exotherm of lopinavir did not show significant change after co-processing (Fig. 2). This thermal behavior suggests development of new crystalline species with mixture containing lopinavir and menthol at 1:2 M ratio being optimum for this transformation. Taking the published data on menthol into consideration, it was expected to have eutectic mixture formation [57,58] but the recorded thermal behavior did not reflect significant reduction in the melting point. Accordingly, the developed crystalline species can be considered as co-crystal of lopinavir with menthol. Menthol induced co-crystallization was reported in few literature reports with some compounds such as lidocaine and xylitol [35,42].

### 3.1.4. X-ray powder diffraction

X-ray diffraction was used to investigate further the nature of the new crystalline species which was assumed to develop based on thermal

analysis after co-processing of lopinavir with menthol. Fig. 3 shows the X-ray diffraction of lopinavir, menthol and their co-processed mixtures. The recorded diffractogram of lopinavir confirms its crystalline nature as revealed from the presence of multiple diffraction peaks at 2θ values of 5.2, 6.7, 7.7, 12.5, 13.2, 15.1, 16.8, 18.3, 19.6, 21.05, 22.4, 26.1°. Similar diffraction pattern for lopinavir was reported in the literature reports [20,55,59]. For pure ground menthol, the diffractogram shows several diffraction peaks at 2θ of 8.2, 9.5, 12.6, 14.3, 15.3, 16.7, 17.3, 19.2, 20.4, 21.8, 22.5°. This diffraction pattern suggests the crystallinity of the ground menthol and complies with the previously published data [50,51].

Wet co-grinding of lopinavir with menthol at increasing molar ratios produced crystalline product with XRD pattern which is different from the sum of diffraction pattern of lopinavir and menthol highlighting the development of new crystalline species. The modulated diffraction pattern was characterized by development of new diffraction peaks at 2θ of 12.5, 13.2, 23 and 23.3 in addition to a change in the relative heights of diffraction peaks. This new pattern was shown in all formulations but that containing lopinavir with menthol at 1:3, molar ratio showed evidence for excess menthol as seen from the appearance of its diffraction peaks. These data confirm the recorded thermal analysis results and supports development of new crystalline species with optimum composition of 1:2, lopinavir to menthol. Additional menthol underwent phase separation. The recorded changes in the X-ray diffraction pattern supports the supposition of co-crystallization between menthol and lopinavir. Similar changes in the diffractograms after coprocessing have been taken as indication for co-crystal formation in literature reports [26,60].

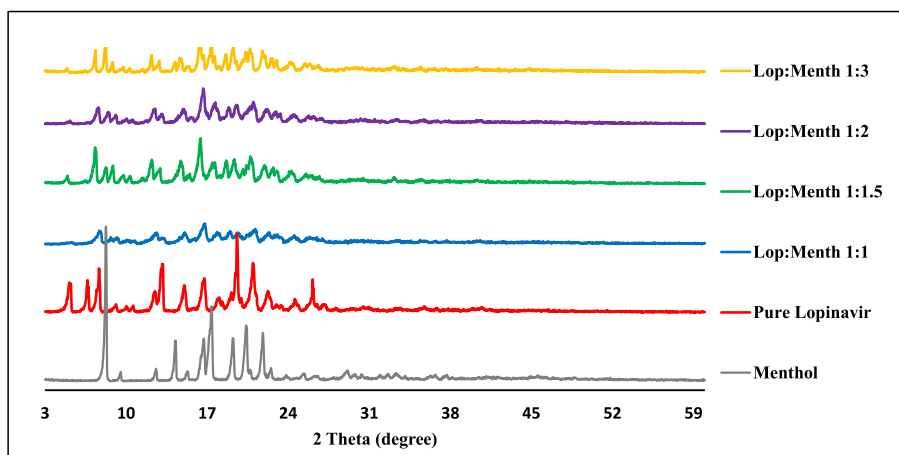


Fig. 3. X-ray diffraction patterns of menthol, pure lopinavir, and formulations containing lopinavir and menthol at molar ratios of 1:1,1:1.5, 1:2, and 1:3.

3.1.5. Dissolution studies

To examine the effect of lopinavir co-processing with menthol on lopinavir dissolution rate, dissolution studies were performed. The resulted dissolution profiles are shown in Fig. 4. These profiles generated the dissolution parameters (DE% and Q5) which are presented in Table 3. For pure untreated lopinavir, the dissolution profile revealed slow and incomplete dissolution with the % dissolved in the first 5 min being 1.56%. The total amount liberated after 1 h was 41.85% of the dose. The overall dissolution efficiency was  $24.96 \pm 1.48\%$ . These values are not acceptable for an immediate release. This slow dissolution rate reflects the hydrophobic nature of lopinavir and correlates with the published work on the drug [16].

Wet co-grinding of lopinavir and menthol resulted in significant enhancement in lopinavir dissolution rate ( $P < 0.01$ ). This enhancement depended on the molar ratio of lopinavir to menthol. The computed % Q5 values for the co-processed mixtures at molar ratio of 1:1, 1:1.5, 1:2, and 1:3 lopinavir to menthol were 26.14, 20.73, 76.55, and 23.45% respectively. The calculated % DE for the same tested formulations were  $50.58 \pm 1.76$ ,  $61.33 \pm 2.83$ ,  $91.43 \pm 0.92$ ,  $44.79 \pm 1.25\%$ . This enhancement in lopinavir dissolution rate in case of the formulations containing lopinavir and menthol at molar ratios of 1:1, 1:1.5, and 1:2 can be accredited to formation of a new crystalline species with weaker crystallinity. Similar behavior was recorded previously with other hydrophobic molecules and are elucidated in the same manner [25,26]. Studying the effect of menthol concentration in the formulation on the dissolution behavior of lopinavir, the dissolution parameters increased with menthol concentrations up to a molar ratio of 1:2 (lopinavir:menthol). Further increase in menthol concentration was associated

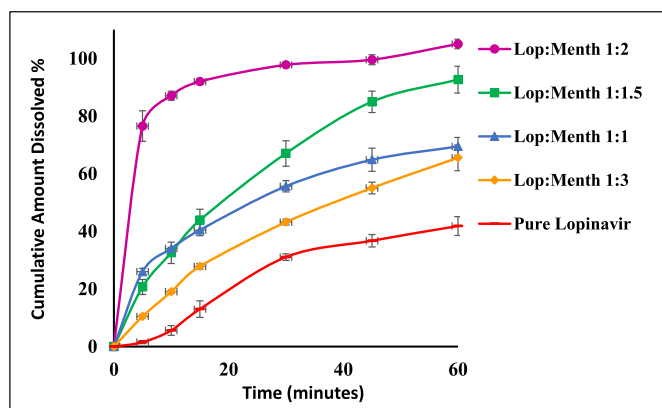


Fig. 4. Dissolution profiles of pure lopinavir, and formulations containing lopinavir and menthol at molar ratios of 1:1,1:1.5, 1:2, and 1:3.

Table 3

The calculated dissolution parameters of lopinavir before and after co-processing with menthol.

Formulation	% Q5	% DE
Pure Lopinavir	1.56 (0.54)	24.96 (1.48)
Lop: Menth 1:1	26.04 (1.12)	50.58 (1.76)
Lop: Menth 1:1.5	20.73 (2.6)	61.33 (2.83)
Lop: Menth 1:2	76.55 (5.32)	91.43 (0.92)
Lop: Menth 1:3	23.45 (5.03)	44.79 (1.25)

Values between brackets are SD, n = 3.

with a decrease in the dissolution parameters compared to the optimum molar ratio (1:2). The similarity factor test reflected the same pattern with formulation containing 1:2 being significantly better than other formulations with respect to dissolution behavior (Table 4). This behavior can be explained taking into consideration the thermal analysis and X-ray diffraction data which indicated possible phase separation of excess menthol. The decrease in dissolution rate at higher concentration of menthol may suggest self-association of menthol after separation of excess menthol. Certain degree of phase separation after co-crystallization has been shown [61].

3.2. In-situ intestinal perfusion of lopinavir

The primary objective of this research was to investigate the effect of co-processing of lopinavir with menthol on the dissolution rate and intestinal absorption of lopinavir. The intestinal absorption was monitored using in-situ intestinal perfusion technique. The rabbit in-situ intestinal perfusion was employed based on previous investigations which

Table 4

The F2 values recorded from the similarity factor test applied to the dissolution data of lopinavir from unprocessed powder or co-processed mixtures with menthol.

Formulation	Pure Lopinavir	Lop: Menth 1:1	Lop: Menth 1:1.5	Lop: Menth 1:2	Lop: Menth 1:3
Pure Lopinavir	-	29	24	5	28
Lop: Menth 1:1	29	-	48	14	34
Lop: Menth 1:1.5	24	48	-	13	22
Lop: Menth 1:2	5	14	13	-	9
Lop: Menth 1:3	28	34	22	9	-

reflected the feasibility of this model in monitoring the intestinal absorption. This model eliminates the effect of food by excluding the stomach. Moreover, the use of rabbit guarantees the presence of similar anatomical and physiological features to human intestine while providing much information about the absorption rate and pathway [48, 49,62,63]. The calculated permeation parameters are presented in Table 5. The effect of water flux on intestinal absorption is shown in Fig. 5.

Perfusion of simple aqueous solution of lopinavir reflected the incomplete absorption from duodenum and jejunum-ileum segments. This incomplete absorption was reflected from the recorded negative values for the ARL which were  $-261.18$ ,  $-240.22$  cm in case of the duodenum and jejunum-ileum, respectively. This was further manifested from the computed L95% values which were 276.18 and 339.54 cm for duodenum and jejunum-ileum, respectively (Table 5). The absorptive clearance normalized to segment length values were ranked as duodenum > jejunum-ileum. This suggests a decrease in the absorptive clearance of lopinavir as we move distally through small intestine. This rank is the reverse of the magnitude of expression of P-gp efflux transporters which are preferentially expressed in the distal parts of small intestine [64–66]. Accordingly, we can postulate that the incomplete absorption of lopinavir can be at least partially due to P-gp efflux mechanism. This postulation correlates with the published data on lopinavir [16–19].

The effect of water flux on the absorptive clearance of lopinavir was investigated to estimate the pathway of lopinavir absorption. This investigation involved plotting the absorptive clearance per unit length as a function of water flux per unit length. Regression analysis of these plots was used to determine the contribution of transcellular and paracellular pathways. These plots are shown in Fig. 5. The intercept with Y axis was taken as a measure for the absorptive clearance at zero water flux which represents the fraction absorbed via transcellular pathway. Comparing this value with the overall absorptive clearance, the contribution of paracellular pathway was estimated. This calculation indicated that 61.7% of the absorption was via transcellular pathway with 38.3% being absorbed via the paracellular pathway in case of duodenum. The dominance of transcellular absorption was clear in case of jejunum-ileum segment with 100% of lopinavir disappearing via transcellular pathway (Table 5 and Fig. 5). The absence of significant effect for water flux on lopinavir absorption from jejunum-ileum was further confirmed by statistical analysis which indicated that the slope of the plot of absorptive clearance as a function of water flux was not significantly different from zero ( $P > 0.05$ , regression analysis).

Co-perfusion of lopinavir with menthol increased the intestinal absorption of lopinavir compared with the corresponding aqueous solution. The absorptive clearance normalized to segment length was increased by 1.6 and 1.3-fold after co-perfusion of lopinavir and menthol at molar ratio of 1:2 in case of duodenum and jejunum-ileum respectively. Statistical analysis of these data revealed the existence of a trend of enhanced absorption after co-perfusion with menthol ( $P > 0.05$ ). This

requires future confirmation with larger number of replicates. This increase in the absorptive clearance was reflected as an increase in the % fraction absorbed (%Fa) in addition to reduction in length required for complete drug absorption (L95%) (Table 5). The increase in absorptive clearance was generally through the transcellular pathway as noticed from the data of the duodenum which showed increased contribution of transcellular pathway after co-perfusion with menthol (Table 5). The recorded enhancement of intestinal permeation can be explained on the base of the intestinal membrane fluidizing effect of menthol. This effect has been suggested in literature reports [37–40,67,68]. The ability of menthol to inhibit the effect of P-gp efflux transporters has been suggested by other investigators [19,41]. However, this effect can not be taken as the main factor contributing to menthol-mediated enhancement in intestinal absorption of lopinavir. This comment is based on the recorded data which reflected better effect for menthol on the absorptive clearance from the duodenum which is believed to have lower magnitude of expression of P-gp transporters compared with the jejunum-ileum.

#### 4. 4. Conclusion

Ethanol assisted kneading of lopinavir with menthol resulted in co-crystal formation with augmented dissolution rate compared with pure lopinavir. The optimum ratio for co-crystallization was 1:2 M ratio of lopinavir and menthol. Formulations containing higher proportions of menthol showed phase separation of menthol due to possible self-association. Co-crystallization with menthol hastened both the dissolution rate, and intestinal permeability of lopinavir. The study introduced menthol for modification of the crystalline structure, enhancing dissolution rate and augmenting intestinal absorption of lopinavir after simple co-processing.

#### Funding

This research did not receive any specific grant from funding agencies in the public, commercial, or not-for-profit sectors.

#### CRediT authorship contribution statement

**Noha D. Fayed:** Investigation, Methodology, Data curation, Visualization, and, Writing – original draft. **Mona F. Arafa:** Methodology, Visualization, Supervision, Writing – review & editing. **Ebtesam A. Essa:** Visualization, Writing – review & editing. **Gamal M. El Maghraby:** Conceptualization, Methodology, Visualization, Supervision, Writing – review & editing.

#### Declaration of competing interest

The authors declare that they have no known competing financial interests or personal relationships that could have appeared to influence

**Table 5**

Membrane transport parameters of lopinavir after perfusion through different segments of rabbit intestine in the form of pure lopinavir or after co-perfusion with menthol at a molar ratio of 1:2 Lop:Menth.

Parameters	Pure Lopinavir		Lop:Menth 1:2	
	Duodenum	Jejunum-ileum	Duodenum	Jejunum-ileum
PeA/L (ml/min.cm)	0.0049 (0.0014)	0.0038 (0.001)	0.008 (0.0008)	0.0049 (0.0014)
Rout/Rin	0.759 (0.068)	0.657 (0.083)	0.609 (0.012)	0.593 (0.06)
L95% (cm)	276.18 (121.5)	339.54 (79.03)	100.92 (13.06)	181.39 (40.87)
%Fa/L (%cm <sup>-1</sup> )	1.61 (0.454)	1.17 (0.27)	2.501 (0.23)	1.397 (0.2123)
JW/L (ml/min.cm)	0.0012 (0.0006)	-0.0002 (0.0007)	0.0024 (0.0004)	0.0002 (0.0006)
ARL (cm)	-261.18	-240.22	-84.92	-152.4
Absorption pathway	Transcellular (%)	61.7	75.2	94.4
	Paracellular (%)	38.3	0	5.6

PeA/L is absorptive clearance normalized to the segment length, Rout/Rin is the fraction remaining after absorption, %Fa/L is the percentage fraction absorbed per unit length, L95% is the required length for 95% absorption, ARLs is the anatomical reserve length and JW/L is the water flux normalized to the segment length. Values between brackets are SEM (n = 3). The percentage of lopinavir absorbed via transcellular and paracellular pathways.

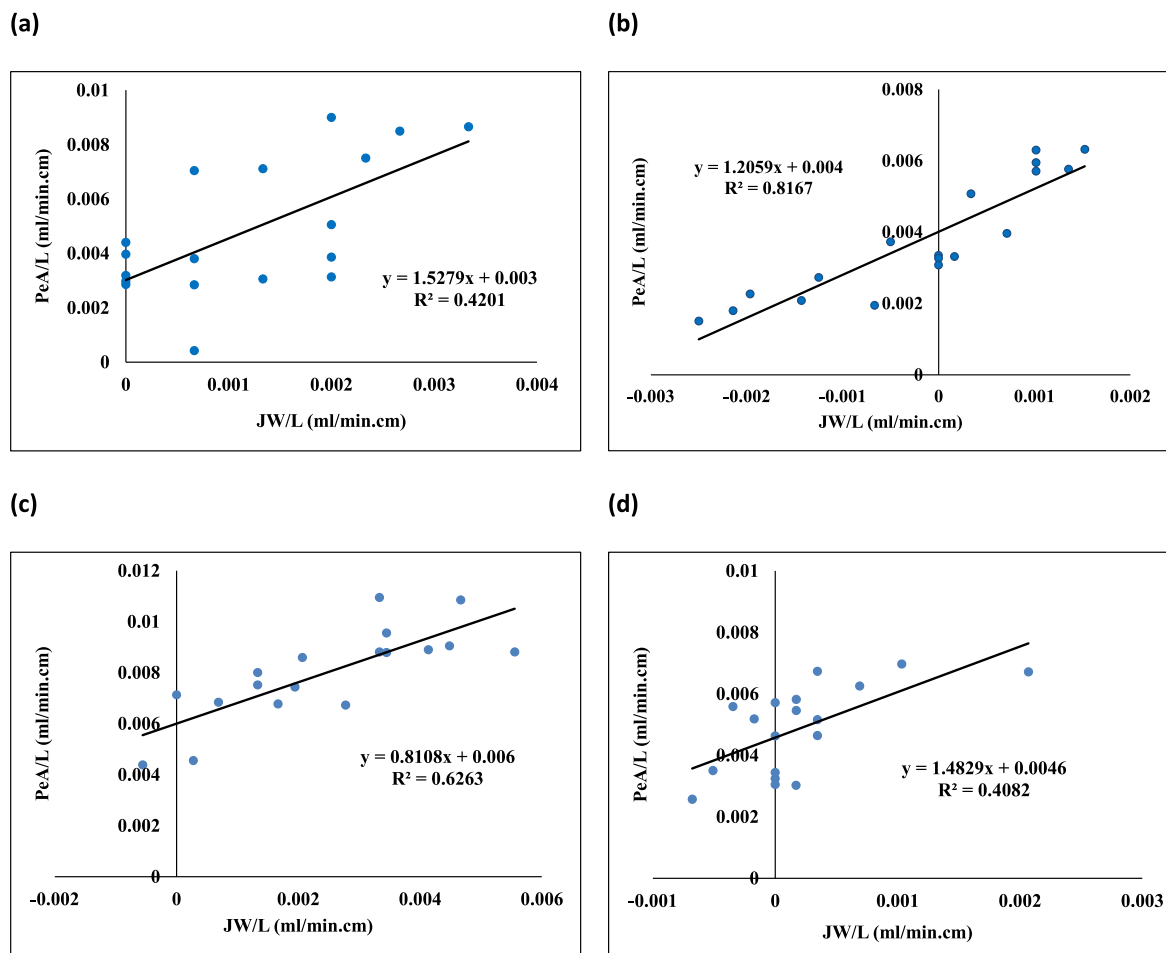


Fig. 5. Absorptive clearance of lopinavir from deudenum (left) and jejuno-ileum (right) as a function of the net water flux. The data obtained after perfusion of aqueous drug solution (a,b), and after co-perfusion with menthol (c,d).

the work reported in this paper.

#### Data availability

Data will be made available on request.

#### References

- [1] H.T. Pham, T. Mesplède, The latest evidence for possible HIV-1 curative strategies, *Drugs Context (US)* 7 (2018), 212522, <https://doi.org/10.7573/dic.212522>.
- [2] A.A. Khan, J. Mudassar, S. Akhtar, V. Murugaiyah, Y. Darwis, Freeze-dried lopinavir-loaded nanostructured lipid carriers for enhanced cellular uptake and bioavailability: statistical optimization, in vitro and in vivo evaluations, *Pharmaceutics* 11 (2019) 97, <https://doi.org/10.3390/pharmaceutics11020097>.
- [3] M.L. Chiu, W.M. Liang, J.P. Li, C.F. Cheng, J.S. Chiou, M.W. Ho, Y.C. Wu, T.H. Lin, C.C. Liao, S.M. Huang, F.J. Tsai, Dosage, and adherence of antiretroviral therapy and risk of osteoporosis in patients with human immunodeficiency virus infection in taiwan: a nested case-control study, *Front. Pharmacol.* 12 (2021), 631480, <https://doi.org/10.3389/fphar.2021.631480>.
- [4] I. Tanaudommongkon, A. Tanaudommongkon, X. Dong, Development of in situ self-assembly nanoparticles to encapsulate lopinavir and ritonavir for long-acting subcutaneous injection, *Pharmaceutics* 13 (2021) 904, <https://doi.org/10.3390/pharmaceutics13060904>.
- [5] C. Fraichard, F. Bonnet-Serrano, C. Laguillier-Morizot, M. Hebert-Schuster, R. Lai-Kuen, J. Sibide, T. Fournier, M. Guibourdenche Cohen, Protease inhibitor anti-HIV, lopinavir, impairs placental endocrine function, *Int. J. Mol. Sci.* 22 (2021) 683, <https://doi.org/10.3390/ijms22020683>.
- [6] S.E. Kandel, J.N. Lampe, Inhibition of CYP3A7 DHEA-S oxidation by lopinavir and ritonavir: an alternative mechanism for adrenal impairment in HIV antiretroviral-treated neonates, *Chem. Res. Toxicol.* 34 (2021) 1150–1160, <https://doi.org/10.1021/acs.chemrestox.1c00028>.
- [7] M. Owor, C. Tierney, L. Ziemba, R. Browning, J. Moye, B. Graham, C. Reding, D. Costello, J. Norman, L. Wiesner, E. Hughes, Pharmacokinetics and safety of zidovudine, lamivudine, and lopinavir/ritonavir in HIV-infected children with severe acute malnutrition in sub-saharan africa: IMPAACT protocol P1092, *J. Pediatr. Infect. Dis.* 40 (2021) 446–452, <https://doi.org/10.1097/INF.0000000000003055>.
- [8] M.Q. Granato, I.S. Sousa, T.L. Rosa, D.S. Gonçalves, S.H. Seabra, D.S. Alviano, M. C. Pessolani, A.L. Santos, L.F. Kneipp, Aspartic peptidase of *Phialophora verrucosa* as target of HIV peptidase inhibitors: blockage of its enzymatic activity and interference with fungal growth and macrophage interaction, *J. Enzym. Inhib. Med. Chem.* 35 (2020) 629–638, <https://doi.org/10.1080/14756366.2020.1724994>.
- [9] A.L. Santos, L.A. Braga-Silva, D.S. Gonçalves, L.S. Ramos, S.S. Oliveira, L.O. Souza, V.S. Oliveira, R.D. Lins, M.R. Pinto, J.E. Muñoz, C.P. Taborda, Repositioning lopinavir, an HIV protease inhibitor, as a promising antifungal drug: lessons learned from *Candida albicans*—in silico, in vitro and in vivo approaches, *J. Fungi* 7 (2021) 424, <https://doi.org/10.3390/jof7060424>.
- [10] K.M. Rebello, V.V. Andrade-Neto, A.A. Zuma, M.C.M. Motta, C.R.B. Gomesde, M.V. N. Souza, G.C. Atella, M.H. Branquinha, A.L. Santos, E.C. Torres-Santos, C. M. d'Avila-Levy, Lopinavir, an HIV-1 peptidase inhibitor, induces alteration on the lipid metabolism of *Leishmania amazonensis* promastigotes, *Parasitology* 145 (2018) 1304–1310, <https://doi.org/10.1017/S0031182018000823>.
- [11] L.S. Sanganito, M.G. Pereira, T. Souto-Pradon, M.H. Branquinha, A.L. Santos, Lopinavir and nelfinavir induce the accumulation of crystalloid lipid inclusions within the reservosomes of *trypanosoma cruzi* and inhibit both aspartyl-type peptidase and cruzipain activities detected in these crucial organelles, *Trav. Med. Infect. Dis.* 6 (2021) 120, <https://doi.org/10.3390/tropicalmed6030120>.
- [12] N. Li, L.S. Taylor, Tailoring supersaturation from amorphous solid dispersions, *J. Contr. Release* 10 (2018) 114–125, <https://doi.org/10.1016/j.jconrel.2018.04.014>.
- [13] L. Chouchana, S. Boujaafar, I. Gana, L.H. Preta, L. Regard, P. Legendre, C. Azoulay, E. Canoui, J. Zerbit, N. Carlier, B. Terrier, Plasma concentrations and safety of lopinavir/ritonavir in COVID-19 patients, *Ther. Drug Monit.* 43 (2021) 131–135, <https://doi.org/10.1097/FTD.0000000000000838>.
- [14] R.N. Dalocchio, A. Dessi, A. De Vito, G. Delogu, P.A. Serra, G. Madeddu, Early combination treatment with existing HIV antivirals: an effective treatment for COVID-19, *Eur. Rev. Med. Pharmacol. Sci.* 25 (2021) 2435–2448, [https://doi.org/10.26355/eurev\\_202103\\_25285](https://doi.org/10.26355/eurev_202103_25285).

- [15] A. Wadaa-Allah, M.S. Emhamed, M.A. Sadeq, N. Ben Hadj Dahman, I. Ullah, N. S. Farrag, A. Negida, Efficacy of the current investigational drugs for the treatment of COVID-19: a scoping review, *Ann. Med.* 53 (2021) 318–334, <https://doi.org/10.1080/07853890.2021.1875500>.
- [16] E.M. Donato, L.A. Martins, P.E. Fröhlich, A.M. Bergold, Development and validation of dissolution test for lopinavir, a poorly water-soluble drug, in soft gel capsules, based on in vivo data, *J. Pharm. Biomed. Anal.* 47 (2008) 547–552, <https://doi.org/10.1016/j.jpba.2008.02.014>.
- [17] S. Jain, J.M. Sharma, A.K. Jain, R.R. Mahajan, Surface-stabilized lopinavir nanoparticles enhance oral bioavailability without coadministration of ritonavir, *Nanomedicine*. (Lond.) 8 (2013) 1639–1655. <https://doi.org/10.2217/nmm.12.181>.
- [18] M. Patel, N. Mandava, M. Gokulgandhi, D. Pal, A.K. Mitra, Amino acid prodrugs: an approach to improve the absorption of HIV-1 protease inhibitor, lopinavir, *Pharmaceuticals* 7 (2014) 433–452. <https://doi.org/10.3390/ph7040433>.
- [19] B. Garg, O.P. Katare, S. Beg, S. Lohan, B. Singh, Systematic development of solid self-nanoemulsifying oily formulations (S-SNEOFs) for enhancing the oral bioavailability and intestinal lymphatic uptake of lopinavir, *Colloids Surf., B* 141 (2016) 611–622, <https://doi.org/10.1016/j.colsurfb.2016.02.012>.
- [20] R. Hamed, E.M. Mohamed, K. Sediri, M.A. Khan, Z. Rahman, Development of stable amorphous solid dispersion and quantification of crystalline fraction of lopinavir by spectroscopic-chemometric methods, *Int. J. Pharm.* 602 (2021), 120657, <https://doi.org/10.1016/j.ijpharm.2021.120657>.
- [21] K. Pham, D. Li, S. Guo, S. Penzak, X. Dong, Development and in vivo evaluation of child-friendly lopinavir/ritonavir pediatric granules utilizing novel in situ self-assembly nanoparticles, *J. Contr. Release* 226 (2016) 88–97. <https://doi.org/10.1016/j.jconrel.2016.02.001>.
- [22] L. Katata-Seru, B.M. Ojo, O. Okubanjo, R. Soremekun, O.S. Aremu, Nanoformulated Eudragit lopinavir and preliminary release of its loaded suppositories, *Heliyon* 6 (2020), e03890, <https://doi.org/10.1016/j.heliyon.2020.e03890>.
- [23] N.S. Trasi, S. Bhujbal, Q.T. Zhou, L.S. Taylor, Amorphous solid dispersion formation via solvent granulation – a case study with ritonavir and lopinavir, *Int. J. Pharm. X* 1 (2019), 100035, <https://doi.org/10.1016/j.ijpx.2019.100035>.
- [24] M. Lal, M. Lai, M. Estrada, C. Zhu, Developing a flexible pediatric dosage form for antiretroviral therapy: a fast-dissolving tablet, *J. Pharmacol. Sci.* 106 (2017) 2173–2177, <https://doi.org/10.1016/j.xphs.2017.05.004>.
- [25] M.F. Arafat, S.A. El-Gizawy, M.A. Osman, G.M. El Maghraby, Sucralose as co-crystal co-former for hydrochlorothiazide: development of oral disintegrating tablets, *Drug Dev. Ind. Pharm.* 42 (2016) 1225–1233. <https://doi.org/10.3109/03639045.2015.1118495>.
- [26] M.F. Arafat, S.A. El-Gizawy, M.A. Osman, G.M. El Maghraby, Xylitol as a potential co-crystal co-former for enhancing dissolution rate of felodipine: preparation and evaluation of sublingual tablets, *Pharmaceut. Dev. Technol.* 23 (2018) 454–463, <https://doi.org/10.1080/10837450.2016.1242625>.
- [27] R.A. Alshaiikh, E.A. Essa, G.M. El Maghraby, Eutectic for enhanced dissolution rate and anti-inflammatory activity of nonsteroidal anti-inflammatory agents: caffeine as a melting point modulator, *Int. J. Pharm.* 563 (2019) 395–405. <https://doi.org/10.1016/j.ijpharm.2019.04.024>. Epub 2019 Apr 9.
- [28] T.K. Mohapatra, A.K. Moharana, R.P. Swain, B.B. Subudhi, Coamorphisation of acetyl salicylic acid and curcumin for enhancing dissolution, anti-inflammatory effect and minimizing gastro toxicity, *J. Drug Deliv. Sci. Technol.* 61 (2021), 102119, <https://doi.org/10.1016/j.jddst.2020.102119>.
- [29] U. Gala, H. Pham, H. Chauhan, Pharmaceutical applications of eutectic mixtures, *J. Develop. Drugs* 2 (2013) 1–2. <https://doi.org/10.4172/2329-6631.1000e130>.
- [30] A.M. Araya-Sibaja, J.R. Vega-Baudrit, T. Guillén-Girón, M. Navarro-Hoyos, S. L. Cuffini, Drug solubility enhancement through the preparation of multicomponent organic materials: eutectics of lovastatin with carboxylic acids, *Pharmaceutics* 11 (2019) 112. <https://doi.org/10.3390/pharmaceutics11030112>.
- [31] A. Alhadid, L. Mokrushina, M. Minceva, Design of deep eutectic systems: a simple approach for preselecting eutectic mixture constituents, *Molecules* 25 (2020) 1077, <https://doi.org/10.3390/molecules25051077>.
- [32] G.C. Bazzo, B.R. Pezzini, H.K. Stulzer, Eutectic mixtures as an approach to enhance solubility, dissolution rate and oral bioavailability of poorly water-soluble drugs, *Int. J. Pharm.* 588 (2020), 119741, <https://doi.org/10.1016/j.ijpharm.2020.119741>.
- [33] A. Alhalaweh, S. George, S. Basavoju, S.L. Childs, S.A. Rizvi, S.P. Velaga, Pharmaceutical cocrystals of nitrofurantoin: screening, characterization, and crystal structure analysis, *CrystEngComm* 14 (2012) 5078–5088. <https://doi.org/10.1039/C2CE06602E>.
- [34] G.L. Perlovich, A.N. Manin, Design of pharmaceutical cocrystals for drug solubility improvement, *Russ. J. Gen. Chem.* 84 (2014) 407–414. <https://doi.org/10.1134/S107036321402042X>.
- [35] E. Stoler, J.C. Warner, Non-Covalent Derivatives: Cocrystals and Eutectics *Molecules* 20 (2015) 14833–14848. <https://doi.org/10.3390/molecules200814833>.
- [36] J. Haneef, R. Chadha, Drug-drug multicomponent solid forms: cocrystal, coamorphous and eutectic of three poorly soluble antihypertensive drugs using mechanochemical approach, *AAPS PharmSciTech* 18 (2017) 2279–2290. <https://doi.org/10.1208/s12249-016-0701-1>.
- [37] L.S. Kang, H.W. Jun, J.W. McCall, Physicochemical studies of lidocaine-menthol binary systems for enhanced membrane transport, *Int. J. Pharm.* 206 (2000) 35–42. [https://doi.org/10.1016/S0378-5173\(00\)00505-6](https://doi.org/10.1016/S0378-5173(00)00505-6).
- [38] C.S. Yong, C.H. Yang, J.D. Rhee, Enhanced rectal bioavailability of ibuprofen in rats by poloxamer 188 and menthol, *Int. J. Pharm.* 269 (2004) 169–176. <https://doi.org/10.1016/j.ijpharm.2003.09.013>.
- [39] T. Narishetty, R. Panchagnula, Effect of L-menthol and 1,8-cineole on phase behavior and molecular organization of SC lipids and skin permeation of zidovudine, *J. Contr. Release* 102 (2005) 59–70, <https://doi.org/10.1016/j.jconrel.2004.09.016>.
- [40] F. Li, J. Peng, Q. Cheng, W. Zhu, Y. Jin, Delivery of 125I-cobrotoxin after intranasal administration to the brain: a microdialysis study in freely moving rats, *Int. J. Pharm.* 328 (2007) 161–167, <https://doi.org/10.1016/j.ijpharm.2006.08.011>.
- [41] N. Silva, L. Salgueiro, A. Fortuna, C. CavaleiroP-glycoprotein mediated efflux modulators of plant origin: a short review, *Nat. Prod. Commun.* 11 (2016) 699–704, <https://doi.org/10.1177/1934578X1601100538>.
- [42] Y. Corvis, P. Négrier, M. Lazerges, S. Massip, J. Léger, P. Espeau, Lidocaine/L-menthol binary system: cocrystallization versus solid-state immiscibility, *J. Phys. Chem. B* 114 (2010) 5420–5426, <https://doi.org/10.1021/jp101303j>.
- [43] T. Phaechamud, S. Tuntarawongsa, Transformation of eutectic emulsion to nanosuspension fabricating with solvent evaporation and ultrasonication technique, *Int. J. Nanomed.* 11 (2016) 2855–2865. <https://doi.org/10.2147/IJN.S108355>.
- [44] R.A. Alshaiikh, E.A. Essa, G.M. El Maghraby, Preparation of stabilized submicron fenofibrate crystals on niacin as a hydrophilic hydrotropic carrier, *Pharmaceut. Dev. Technol.* 25 (2020) 168–177. <https://doi.org/10.1080/10837450.2019.1682609>.
- [45] K.A. Khan, The concept of dissolution efficiency, *J. Pharm. Pharmacol.* 27 (1975) 48–49. <https://doi.org/10.1111/j.2042-7158.1975.tb09378.x>.
- [46] M.C. Gohel, G. Sarvaiya, R. Shah, K. Brahmabhatt, Mathematical approach for the assessment of similarity factor using a new scheme for calculating weight, *Indian J. Pharmaceut. Sci.* 71 (2009) 142–144. <https://doi.org/10.4103/0250-474X.54281>.
- [47] L.E. Riad, R.J. Sawchuk, Absorptive clearance of carbamazepine and selected metabolites in rabbit intestine, *Pharm. Res. (N. Y.)* 8 (1991) 1050–1055. <https://doi.org/10.1023/a:1015817426713>.
- [48] M.A. Osman, G.M. El Maghraby, M.A. Hedayat, Intestinal absorption and presystemic disposition of sildenafil citrate in the rabbit: evidence for site dependent absorptive clearance, *Biopharm. Drug Dispos.* 27 (2006) 93–102, <https://doi.org/10.1002/bdd.487>.
- [49] A.A. Sultan, S.A. El-Gizawy, M.A. Osman, G.M. El Maghraby, Colloidal carriers for extended absorption window of furosemide, *J. Pharm. Pharmacol.* 68 (2016) 324–332. <https://doi.org/10.1111/jphp.12516>.
- [50] M.G. Maniyar, C.R. Kokare, Formulation and evaluation of spray dried liposomes of lopinavir for topical application, *J. Pharm. Investig.* 49 (2019) 259–270, <https://doi.org/10.1007/s40005-018-0403-7>.
- [51] M.K. Trivedi, S. Patil, R. Mishra, S. Jana, Structural and physical properties of biofield treated thymol and menthol, *J. Mol. Pharm. Org. Process. Res.* 3 (2015), 1000127, <https://doi.org/10.4172/2329-9053.1000127>.
- [52] Z.I. Yildiz, A. Celebioglu, M.E. Klicic, E. Durgun, T. Uyar, Menthol/cyclodextrin inclusion complex nanofibers: enhanced water solubility and high-temperature stability of menthol, *J. Food Eng.* 224 (2018) 27–36, <https://doi.org/10.1016/j.jfoodeng.2017.12.020>.
- [53] A. Abri, N. Babajani, A.M. Zonouz, H. Shekaari, Spectral and thermophysical properties of some novel deep eutectic solvent based on l-menthol and their mixtures with ethanol, *J. Mol. Liq.* 285 (2019) 477–487, <https://doi.org/10.1016/j.jmolliq.2019.04.001>.
- [54] M.A. Alex, A.J. Chacko, S. Jose, E.B. Souto, Lopinavir loaded solid lipid nanoparticles (SLN) for intestinal lymphatic targeting, *Eur. J. Pharmaceut. Sci.* 42 (2011) 11–18, <https://doi.org/10.1016/j.ejps.2010.10.002>.
- [55] A. Shinde, N. Jadhav, H. More, H. Naikwad, Design and characterisation of lopinavir nanocrystals for solubility and dissolution enhancement, *Pharm. Sci. Asia* 46 (2019) 193–205. <https://doi.org/10.29090/psa.2019.03.018.0020>.
- [56] Y. Sun, S. Fan, R. Liang, X. Ni, Y. Du, J. Wang, C. Yang, Design and characterization of starch/solid lipids hybrid microcapsules and their thermal stability with menthol, *Food Hydrocolloids* 116 (2021), 106631, <https://doi.org/10.1016/j.foodhyd.2021.106631>.
- [57] C.S. Yong, Y.K. Oh, S.H. Jung, J.D. Rhee, H.D. Kim, C.K. Kim, H.G. Choi, Preparation of ibuprofen-loaded liquid suppository using eutectic mixture system with menthol, *Eur. J. Pharmaceut. Sci.* 23 (2004) 347–353. <https://doi.org/10.1016/j.ejps.2004.08.008>.
- [58] F. Al-Akayleh, H.H.M. Ali, M.M. Ghareeb, M. Al-Remawi, Therapeutic deep eutectic system of capric acid and menthol: characterization and pharmaceutical application, *J. Drug Deliv. Sci. Technol.* 53 (2019), 101159, <https://doi.org/10.1016/j.jddst.2019.101159>.
- [59] H.S. Mahajan, P.H. Patil, Central composite design-based optimization of lopinavir vitamin E-TPGS micelle: in vitro characterization and in vivo pharmacokinetic study, *Colloids Surf., B* 194 (2020), 111149, <https://doi.org/10.1016/j.colsurfb.2020.111149>.
- [60] E.A. Essa, A.R. Elbasuony, A.E. Abdelaziz, G.M. El Maghraby, Co-crystallization for enhanced dissolution rate of biclutamide: preparation and evaluation of rapidly disintegrating tablets, *Drug Dev. Ind. Pharm.* 45 (2019) 1215–1223. <https://doi.org/10.1080/03639045.2019.1571504>.
- [61] A.T. Jones, Cocrystallization in copolymers of  $\alpha$ -olefins II—butene-1 copolymers and polybutene type II/I crystal phase transition, *polymer* 7 (1966) 23–59, [https://doi.org/10.1016/S0032-3861\(66\)80015-0](https://doi.org/10.1016/S0032-3861(66)80015-0).
- [62] C.A. Loehry, Small intestine permeability in animal and man, *Gut* 14 (1973) 683–688, <https://doi.org/10.1136/gut.14.9.683>.
- [63] T. Maeda, Use of rabbits for GI drug absorption studies, *J. Pharmacol. Sci.* 66 (1977) 69–73, <https://doi.org/10.1002/jps.260066017>.
- [64] R.H. Stephens, J. Tanianis-Hughes, N.B. Higgs, M. Humphrey, G. Warhurst, Region-dependent modulation of intestinal permeability by drug efflux transporters: in vitro studies in mdr1a (–/–) mouse intestine, *J. Pharmacol. Exp. Therapeut.* 303 (2002) 1095–1101, <https://doi.org/10.1124/jpet.102.041236>, 2002.

- [65] S. Mouly, M.F. Paine, P-glycoprotein increases from proximal to distal regions of human small intestine, *Pharm. Res. (N. Y.)* 20 (2003) 1595–1599, <https://doi.org/10.1023/a:1026183200740>.
- [66] S.M. Ashmawy, S.A. El-Gizawy, G.M. El Maghraby, M.A. Osman, Regional difference in intestinal drug absorption as a measure for the potential effect of P-glycoprotein efflux transporters, *J. Pharm. Pharmacol.* 71 (2019) 362–370, <https://doi.org/10.1111/jphp.13036>.
- [67] Y. Kaplun-Frischoff, E. Touitou, Testosterone skin permeation enhancement by menthol through formation of eutectic with drug and interaction with skin lipids, *J. Pharmacol. Sci.* 86 (1997) 1394–1399, <https://doi.org/10.1021/js9701465>.
- [68] A.H. Shojaei, M. Khan, G. Lim, R. Khosravan, Transbuccal permeation of a nucleoside analog, dideoxycytidine: effects of menthol as a permeation enhancer, *Int. J. Pharm.* 192 (1999) 139–146, [https://doi.org/10.1016/S0378-5173\(99\)00301-4](https://doi.org/10.1016/S0378-5173(99)00301-4).